Generation of Third Code and Phase Signals Based on Dual-Frequency GPS Measurements

Bofeng Li
Tongji University, Shanghai, P.R. China
Queensland University of Technology, Queensland, Australia

BIOGRAPHY

Bofeng Li is a PhD candidate in Department of Surveying and Geo-informatics Engineering, Tongji University, P. R. China. He received BSC degree in Surveying Engineering from Tongji University in 2005. He is currently conducting visiting studies at Faculty of Information Technology, Queensland University of Technology, Australia. His research interests include Network-based positioning algorithms, three carrier ambiguity resolutions, geodetic theory and surveying data processing. Bofeng has received several awards from Tongji University and some other academic organizations for his academic excellence. He is now a membership of IAG working group 4.5.4 for "Data Processing of Multiple GNSS Signals". He has published more than ten journal articles in GPS fields since 2006.

ABSTRACT

Future Global Navigation Satellite Systems (GNSS) will transmit three or more frequency signals, which can potentially benefit rapid and reliable phase ambiguity resolution. Due to the lack of third frequency data, current studies using multiple GNSS signals, such as Three Carrier Ambiguity Resolution (TCAR), are limited to the theoretical analysis based on purely simulated three frequency signals. The problem is that the simulated GNSS data sets, regardless of being generated by an expensive signal generator or a software tool, are not realistic representation of the real world situations. Signals are simulated and data generated based on various assumptions for signal delays, error sources, and uncertainty levels. Thus, these data sets could be very different to that experienced in the real world. In this paper, a new so-called semi-simulation method for generating the third frequency double differenced GPS signals is proposed. The key of this method is the separation between ionospheric biases and geometric errors consisting of three main procedures. In step 1, the integer ambiguities at two frequencies are fixed to their integer values and the geometric and ionospheric biases are separated by means of corresponding combined measurements. This idea is similar to that of the network-based RTK processing. In the second procedure, a new multiple-difference based method is introduced to assess the uncertainties of code and phase measurements as well as the cross correlation between L1 and L2 phase signals for long distance baselines. These stochastic characteristics will be utilized in the generation of random noise components for the new signals. Finally, the third frequency signals are generated according to the proposed procedures based on the separated biases and their stochastic characteristics obtained from the real dual-frequency GPS measurements. The third frequency GPS data sets are generated with baselines of 15, 53 and 78 km in length and further employed for ambiguity resolution and position estimation analysis. The results from these testing baselines have shown consistency with the theoretical analysis. The semi-simulation method is a convenient and efficient alternative for generating the new double differenced third frequency signal based on the existing dual-frequency GPS signals. It will provide benefits to researches and developments for future generation GNSS technology and applications.

INTRODUCTION

Future Global Navigation Satellite Systems (GNSS) will transmit three or more frequency signals. The GPS (Global Positioning Systems) introduced the L5 signal (1176.45MHz) in addition to the current L1 (1575.42MHz) and L2 (1227.6MHz). The Galileo system is designed to provide signals centered at L1 (1575.42MHz), E6 (1278.75MHz), E5B (1207.14MHz) and E5A (1176.45MHz) for commercial and civilian use. The Chinese COMPASS navigation satellite system will transmit four L-band frequency signals at E1 (1589.742 MHz), E2 (1561.098 MHz), E6 (1268.52MHz) and E5B (1207.14 MHz). Additionally, regional satellite system such as Japanese QZSS operates the same three frequencies as GPS. Most of researchers believe that the addition of the signal frequencies will bring benefits to GNSS technology and applications. One of the major benefits believed is that the employment of additional carriers can significantly enhance the performance and reliability of carrier phase Ambiguity Resolution (AR) for longer inter-receiver distances, which is crucial to implementation of real time highly precise positioning at local, regional and global scales with future GNSS constellations (Feng & Rizos 2005; Feng 2008; Hatch et al. 2000).

Extensive studies have thus far been made towards the improvement of AR reliability using dual-frequency GPS data instantaneously (Frei & Beulter 1990; Hatch 1990; Teunissen 1994; Park et al. 1996; Shen & Li 2007). Unfortunately, the reliability and availability of AR and

RTK solutions obtained from the current GPS dual-frequency measurement with a single epoch data are usually in doubt. In addressing carrier AR with three or more signals, the earliest studies by Forssell et al. (1997) and Vollath et al. (1998) described Three Carrier Ambiguity Resolution (TCAR) method. Hatch et al. (2000) proposed the Cascading Ambiguity Resolution (CAR) method. Both of the early TCAR and CAR methods use essentially the identical geometry-free bootstrapped procedure (Teunissen et al. 2002). Werner and Winkel (2003) followed the same TCAR geometry-free analysis and illustrated the success rate results for Galileo case. More recently, Li and Shen (2008) gave out several optimal combinations of Galileo inter-frequencies based on the different objective functions and constraints. Furthermore, they recommended a set of independent optimal combinations for potential epochwise AR. Ji et al. (2007) also presented a set of combinations of Galileo inter-frequencies and compared their success rates of epochwise AR with CAR and LAMBDA (Least squares AMBiguity Decorrelation Adjustment) methods. Cao et al. (2007) studied the probability of correct fix of ambiguities based on the probabilistic formula of bootstrapped solution as the lower probabilistic bound of LAMBDA. However, Xu (2006) had pointed out this probabilistic formula is incorrect. Feng (2008) proposed geometry-based TCAR using ionosphere-reduced virtual signals and also analyzed the success rate for instantaneous AR. To sum up, all of the above methods are due to the choice of optimal combinations of multiple frequency signals for which are related to longer wavelength or/and reduced ionospheric delay and other beneficial properties.

Due to the lack of the third frequency measurements, existing TCAR studies are limited to the theoretical and numerical analysis with dual-frequency GPS data or purely simulated three carrier data generated by either signal generator or a software tool. The results from dual-frequency GPS data can not demonstrate full performance potential of the additional carrier signals, while results from the purely simulated data can only show the influences on AR and position estimation relative to different levels of phase and code uncertainties. It is, however, too difficult to simulate real world scenarios under the different ionospheric and tropospheric biases due to their complex spatial and temporal variations. For instance, the factors contributing to the tropospheric delay include time, location, vapour, temperature and so on.

In this research, we will attempt to provide a new method, namely semi-simulation method for generating additional signals based on GPS dual-frequency data. In principle, one can reserve the consistent systematic errors and introduce additional observational noises to the third frequency signals. The key is to separate the effects of ionospheric and tropospheric errors from the noised Double Differenced (DD) measurements. Similarly to the algorithms used in network-based RTK, the ionospheric and tropospheric biases at DD code and phase measurements can be obtained. These biases are substituted into the third signals, while the code and phase noises of the third signals are generated by analysing their stochastic characteristics from dual-frequency data. It is anticipated that the newly semi-simulated three frequency data can objectively reflect the real world situation and thus more suitable for TCAR and position estimation analysis, especially for the performance improvement with respect to the dual-frequency cases. Although initially developed for generating the third GPS frequency signals, this semi-simulation method can trivially be extended to the generation of other L-band signals for other GNSS satellite systems.

The semi-simulation method for generating the third frequency signals based on the existing dual-frequency GPS data generally involves several major procedures. i) Estimate DD ambiguities of the baseline and separate the geometric errors and ionospheric delays in the DD measurements; ii) Evaluate the stochastic characteristics including uncertainties of code and phase noises and cross correlation between L1 and L2 phases, in order to provide the statistical parameters for generating new signals; iii) Generate the third frequency signals according to the above biases and errors; and iv) Validate the TCAR and position estimation using the generated signals, which, in turn, reflects the correctness of new signals.

Following sections of the paper is organised as bellows. Section 2 presents the general mathematic models for undifferenced and differenced GPS code and phase signals. Section 3 outlines the generation procedures of the third frequency signals in detail, including a new approach for cross correlation estimation. In Section 4, the data set from a baseline with severe ionospheric disturbance from Guangzhou CORS network of China is firstly examined to show the generation procedure. Additionally, more data sets from the US CORS network are processed and analysed as well to validate the efficiency of the semi-simulation method and the consistency between the theoretical prediction and numerical results of TCAR processing. The research findings are summarized in the last section to finish the paper.

FUNDAMENTAL GPS OBSERVATION MODELS

Considering the satellite and receiver clock biases and various propagation delays, the observation equations of dual-frequency code P_1 , P_2 and phase Φ_1 , Φ_2 can be expressed as,

$$P_1 = \rho + c\left(\delta t_{R,1} - \delta t_{S,1}\right) + \delta_{orbit} + \delta_{trop} + \frac{K}{f_1^2} + \varepsilon_{P_1} \qquad (1a)$$

$$P_2 = \rho + c\left(\delta t_{R,2} - \delta t_{S,2}\right) + \delta_{orbit} + \delta_{trop} + \frac{K}{f_2^2} + \varepsilon_{P_2} \qquad (1b)$$

$$\Phi_1 = \rho + c\left(\delta t_{R,1} - \delta t_{S,1}\right) + \delta_{orb} + \delta_{tro} - \frac{K}{f_1^2} - \lambda_1\left(\varphi_S^0 - \varphi_{R,1}^0 + N_1\right) + \varepsilon_{\Phi_1} \qquad (1c)$$

$$\Phi_2 = \rho + c\left(\delta t_{R,2} - \delta t_{S,2}\right) + \delta_{orb} + \delta_{tro} - \frac{K}{f_2^2} - \lambda_2\left(\varphi_S^0 - \varphi_{R,2}^0 + N_2\right) + \varepsilon_{\Phi_2} \quad (1d)$$

where,

ρ: geometric distance between satellite S and receiver R antenna;

c: speed of light in vacuum;

$\delta t_{R,1}$ and $\delta t_{R,2}$: receiver clock errors in seconds for L1 and L2 frequency respectively;

$\delta t_{S,1}$ and $\delta t_{S,2}$: satellite clock errors in seconds for L1 and L2 frequency respectively;

δ_{orb}: satellite orbital error in meters;

δ_{tro}: tropospheric propagation delay in meters;

φ_S^0: initial phase of the satellite oscillator in cycles, which is satellite-dependent;

$\varphi_{R,1}^0$ and $\varphi_{R,2}^0$: initial phase of the oscillator in cycles respectively for L1 and L2 frequency;

λ_1 and λ_2: wavelengths of L1 and L2 phase;

K: parameter of the first-order ionospheric delay;

N_1 and N_2: integer ambiguities for L1 and L2 phase;

ε_{P_1}, ε_{P_2}, ε_{Φ_1} and ε_{Φ_2}: observation noises with respect to P_1, P_2, Φ_1 and Φ_2 including multipath, residual ionospheric delay (e.g. higher-order ionospheric effect and ionospheric scintillation and receiver system noise (Kim & Langley 2007).

The group ionospheric delay in code measurements (1a) and (1b) and the phase ionospheric delay in (1c) and (1d) have the same magnitude, but in opposite signs. After double difference operation, the code and phase observation Eqs.(1a-1d) become:

$$\Delta P_1 = \Delta\rho + \Delta\delta_{orb} + \Delta\delta_{tro} + \frac{\Delta K}{f_1^2} + \varepsilon_{\Delta P_1} \quad (2a)$$

$$\Delta P_2 = \Delta\rho + \Delta\delta_{orb} + \Delta\delta_{tro} + \frac{\Delta K}{f_2^2} + \varepsilon_{\Delta P_2} \quad (2b)$$

and

$$\Delta\Phi_1 = \Delta\rho + \Delta\delta_{orb} + \Delta\delta_{tro} - \frac{\Delta K}{f_1^2} - \lambda_1\Delta N_1 + \varepsilon_{\Delta\Phi_1} \quad (2c)$$

$$\Delta\Phi_2 = \Delta\rho + \Delta\delta_{orb} + \Delta\delta_{tro} - \frac{\Delta K}{f_2^2} - \lambda_2\Delta N_2 + \varepsilon_{\Delta\Phi_2} \quad (2d)$$

where the symbol "Δ" represents the DD operation product applied right to the quantity immediately; all variables are as defined in Eqs.(1a-1d). It is important to note that not all of the parameters in Eqs.(1a-1d) can be estimated because of the dependence of these parameters. In addition, the undifferenced Eqs.(1a-1d) and the DD Eqs.(2a-2d) are exactly equivalent in terms of position solution (Schaffrin & Grafarend 1986; Shen & Xu 2008).

For convenience, we define the term "geometric error" as follows,

$$\Delta G = \Delta\delta_{orb} + \Delta\delta_{tro} \quad (3)$$

which is common for all types of code and phase observables in Eqs.(2a-2d).

GENERATION OF THE THIRD FREQUENCY GPS SIGNALS

It is noticed that the ionospheric delay, ambiguity and observation noise are dependent on the different frequency observables, whereas the other terms are free of this effect. Therefore, in order to create new frequency observation, the ionospheric delay and geometric error terms must be separately determined in advance. This is different from the single-based RTK processing, where the joint ranging error, including the geometric effect, ionospheric delay and observation noises for L1 and L2 frequencies, are calculated without separating the ionospheric delay from geometric error and phase noise. On the other hand, in the network-based RTK processing, dual-frequency phase ambiguities must be primarily fixed to their integer values in order to separate geometric error and ionospheric delay. For the AR of the network-based RTK operational purpose, we refer to Chen et al. (2001), Hu et al. (2003) and Zhang and Lachapelle (2001), without extension in this context.

In this section, we will first study how to separate geometric error and ionospheric delay from DD observation Eqs.(2a-2d) with the fixed L1 and L2 integers. Next we analyse stochastic characteristics of the signals, including the variances of code and phase and the cross correlation between L1 and L2 phase, which will contribute to simulate the random noise of the generated signal. The generation strategy of the third frequency GPS signals will also be elaborated at the end of this section.

Geometric error and ionospheric delay separation

Once the integer ambiguities for L1 and L2 are fixed, the ionospheric delay at L1 and the geometric error can be derived from Eqs.(2a-2d) and (3) respectively,

$$\frac{\Delta K}{f_1^2} = \Delta I - \frac{f_2^2}{f_1^2 - f_2^2}\left(\varepsilon_{\Delta\Phi_1} - \varepsilon_{\Delta\Phi_2}\right) \quad (4a)$$

where

$$\Delta I = \frac{f_2^2}{f_1^2 - f_2^2}\left(\Delta\Phi_1 - \Delta\Phi_2 + \lambda_1\Delta N_1 - \lambda_2\Delta N_2\right) \quad (4b)$$

and

$$\Delta G = \Delta T - \frac{f_1^2\varepsilon_{\Delta\Phi_1} - f_2^2\varepsilon_{\Delta\Phi_2}}{f_1^2 - f_2^2} \quad (5a)$$

where

$$\Delta T = \frac{f_1^2\Delta\Phi_1 - f_2^2\Delta\Phi_2 + cf_1\Delta N_1 - cf_2\Delta N_2}{f_1^2 - f_2^2} - \Delta\rho \quad (5b)$$

Both the ionospheric term (4a) and the geometric term (5a) contain the effects of phase noises. In the network-based RTK processing, these noised ionospheric errors and geometric biases are interpolated with their individual

functions, providing to rover users for corrections. In generation of the third signals, the effects of the phase noises in (4a) and (5a) must be carefully considered to give the third signals with appropriate order of phase noises. It is important to note that although the tropospheric delay can hardly be separated from the defined geometric terms, this separation is unnecessary at all in the case of generating the third frequency data.

Analysis of the stochastic characteristics

In this subsection, we focus on the evaluation of noise characteristics of dual-frequency phase and code measurements as well as the cross correlation between L1 and L2 phases. By considering the effects of phase noises on the ionospheric and geometric terms, it is aimed to quantify the noise terms to be added to the third signals.

It is desirable to eliminate the systematic errors as much as possible in order to correctly evaluate the stochastic characteristics of GPS measurements, because the systematic errors can seriously contaminate the random noises and thus bias the estimators. In general, the observables collected from zero or ultra-short baselines are employed where the joint effects of geometric and ionospheric errors can be basically ignored (Li et al. 2008). The challenge now is to extract the phase noise characteristics from the DD residuals over longer baselines where the significant systematic errors exist. However, it is possible to overcome the effects of residual systematic errors in an observation series by multiple differencing the DD observations in time domain, e.g. applying triple, quadruple differencing and so on. Through these multiple difference operation, the random noises are enlarged and the systematic errors are almost completely eliminated. The idea may be traced back to Kim and Langley (2001), who also presented a method to determine the order of the differencing based on spectrum analysis. Kim and Langley (2001) showed that all residual systematic errors can be basically eliminated by quadruple differencing for all scenarios, e.g. static, low and high kinematic applications. In this context, we always assume the sample interval of 1 second and the baseline length of a few tens of kilometres for allowing the residual DD systematic errors to be basically eliminated by quadruple differencing operation.

Starting with the Eq. (2c) for DD L1 signals, the triple differenced (TD) observation equation for one epoch is derived by differencing DD measurements at two consecutive epochs,

$$\Delta\dot{\Psi}^t = \Delta\dot{G}^t - \frac{\Delta\dot{K}^t}{f_1^2} + \varepsilon_{\Delta\Phi}^t \tag{6}$$

where

$\Delta\dot{\Psi}^t = \Delta\dot{\Phi}^t - \Delta\dot{\rho}^t$: the equivalent TD phase at L1;

$\Delta\dot{\Phi}^t = \Delta\Phi^{t+1} - \Delta\Phi^t$: the TD phase at L1;

$\Delta\dot{\rho}^t = \Delta\rho^{t+1} - \Delta\rho^t$: the TD geometric distance;

$\Delta\dot{G}^t = \Delta G^{t+1} - \Delta G^t$: the TD geometry error;

$\frac{\Delta\dot{K}^t}{f_1^2} = \frac{\Delta K^{t+1}}{f_1^2} - \frac{\Delta K^t}{f_1^2}$: the TD ionosphere delay at L1;

$\varepsilon_{\Delta\Phi}^t = \varepsilon_{\Delta\Phi}^{t+1} - \varepsilon_{\Delta\Phi}^t$: the TD observation noise;

The superscripts denote the time epochs t+1 and t. Continuing to difference the TD observations of two consecutive epochs, the Quadruple Differenced (QD) observation equation is obtained as,

$$\Delta\ddot{\Psi}^t = \varepsilon_{\Delta\Phi}^{t+2} - 2\varepsilon_{\Delta\Phi}^{t+1} + \varepsilon_{\Delta\Phi}^t \tag{7}$$

where $\Delta\ddot{\Psi}^t = \Delta\dot{\Psi}^{t+1} - \Delta\dot{\Psi}^t$, computed from the observations and geometric distances. After these operations, all the biases are supposedly removed in Eq.(7) except for the effects of random DD phase noises of three consecutive epochs. As a result, the STandard Deviation (STD) of DD phase noise at L1 is calculated with assumption that DD L1 measurements of these three consecutive epochs have the same variance by,

$$\hat{\sigma}_{\Delta\Phi} = \sqrt{\boldsymbol{\Delta\ddot{\Psi}}^T \mathbf{Q}_{\Delta\ddot{\Psi}}^{-1} \boldsymbol{\Delta\ddot{\Psi}} / n} \tag{8a}$$

Here $\boldsymbol{\Delta\ddot{\Psi}} = \left(\Delta\ddot{\Psi}^1 \;\; \Delta\ddot{\Psi}^2 \;\; \cdots \;\; \Delta\ddot{\Psi}^n\right)^T$ is the n-by-1 QD observation vector for one epoch with n DD phase measurements; $\mathbf{Q}_{\Delta\ddot{\Psi}}$ is n-by-n cofactor matrix of QD observations for one epoch and satisfied with,

$$\mathbf{Q}_{\Delta\ddot{\Psi}} = 6\mathbf{Q}_{\Delta\Phi} \tag{8b}$$

where $\mathbf{Q}_{\Delta\Phi}$ is the n-by-n cofactor matrix for DD observations of one epoch.

The next notable issue is whether the cross correlation between L1 and L2 phase noises should be considered in order to generate realistic random noises for the third frequency signals. Li et al. (2008) demonstrated that this cross correlation may vary between receiver types. However, it is less understood both analytically and numerically so far for long baselines. In the following, a new method is developed to estimate the cross correlation based on the QD first-order ionospheric delay. From Eq.(4), the nominal DD ionospheric delay can be directly calculated in Eq.(9),

$$\Delta I = \frac{\Delta K}{f_1^2} + 1.55\left(\varepsilon_{\Delta\Phi_1} - \varepsilon_{\Delta\Phi_2}\right) \tag{9}$$

where the coefficient of combined phase noise is calculated by $f_2^2 / \left(f_1^2 - f_2^2\right) \approx 1.55$. Analogically, the QD operation is carried out to eliminate the first right term of Eq.(9) between epochs. The QD observation of the ionospheric delay reads,

$$\Delta\ddot{I}^t = 1.55\left(\varepsilon_{\Delta\Phi_{1,-1}}^{t+2} - 2\varepsilon_{\Delta\Phi_{1,-1}}^{t+1} + \varepsilon_{\Delta\Phi_{1,-1}}^t\right) \tag{10}$$

where $\varepsilon_{\Delta\Phi_{1,-1}} = \varepsilon_{\Delta\Phi_1} - \varepsilon_{\Delta\Phi_2}$. We can estimate the STD of combined phase noise $\varepsilon_{\Delta\Phi_{1,-1}}$ similarly as before by,

$$\hat{\sigma}_{\Delta\Phi_{1,-1}} = \frac{\sqrt{\Delta\ddot{\mathbf{I}}^{T}\mathbf{Q}_{\Delta\ddot{\Psi}}^{-1}\Delta\ddot{\mathbf{I}}/n}}{1.55} \quad (11)$$

where $\Delta\ddot{\mathbf{I}} = \left(\Delta\ddot{I}^{1} \quad \Delta\ddot{I}^{2} \quad \cdots \quad \Delta\ddot{I}^{n}\right)^{T}$. In principle, the STD of $\varepsilon_{\Delta\Phi_{1,-1}}$ is satisfied with the following relationship,

$$\sigma^2_{\Delta\Phi_{1,-1}} = \sigma^2_{\Delta\Phi_1} + \sigma^2_{\Delta\Phi_2} - 2\rho_{\Phi_1,\Phi_2}\sigma_{\Delta\Phi_1}\sigma_{\Delta\Phi_2} \quad (12)$$

where $\sigma_{\Delta\Phi_1}$ and $\sigma_{\Delta\Phi_2}$ can be determined by Eq.(8). Therefore, the cross correlation coefficient is derived as,

$$\hat{\rho}_{\Phi_1,\Phi_2} = \frac{\hat{\sigma}^2_{\Delta\Phi_1} + \hat{\sigma}^2_{\Delta\Phi_2} - \hat{\sigma}^2_{\Delta\Phi_{1,-1}}}{2\hat{\sigma}_{\Delta\Phi_1}\hat{\sigma}_{\Delta\Phi_2}} \quad (13)$$

One now can estimate the STD of DD codes. Inserting (4) and (5) into (2a), we can derive an alternative form of the DD P1 code observation equation,

$$\Delta P_1 = \Delta\rho + \Delta T + \Delta I + \varepsilon_{\Delta P_1} - 4.09\varepsilon_{\Delta\Phi_1} + 3.09\varepsilon_{\Delta\Phi_2} \quad (14)$$

where the coefficients of $\varepsilon_{\Delta\Phi_1}$ and $\varepsilon_{\Delta\Phi_2}$ are calculated by $\left(f_1^2 + f_2^2\right)/\left(f_1^2 - f_2^2\right) \approx 4.09$ and $2f_2^2/\left(f_1^2 - f_2^2\right) \approx 3.09$. Comparing (14) with (6), all of the systematic errors are completely eliminated no matter of the baseline lengths and how the combined phase noise are introduced. Although the phase accuracy is much higher than that of the code, the phase noises are enlarged and should be removed to correctly estimating the STD of code. The procedure for estimating STD of DD code observation is as follows. Firstly, the residuals of (14) are calculated by,

$$v_{P\Phi} = \Delta P_1 - \Delta\rho - \Delta T - \Delta I \quad (15)$$

and thus STD can be determined by,

$$\hat{\sigma}_{\Delta P_1} = \sqrt{\hat{\sigma}^2_{P\Phi} - \hat{\sigma}^2_{\Delta\Phi_C}} \quad (16a)$$

where

$$\hat{\sigma}_{P\Phi} = \sqrt{\mathbf{v}_{P\Phi}^{T}\mathbf{Q}_{\Delta\Phi}^{-1}\mathbf{v}_{P\Phi}/n} \quad (16b)$$

and

$$\hat{\sigma}^2_{\Delta\Phi_C} = 16.74\hat{\sigma}^2_{\Delta\Phi_1} + 9.55\hat{\sigma}^2_{\Delta\Phi_2} - 25.28\hat{\rho}_{\Phi_1,\Phi_2}\hat{\sigma}_{\Delta\Phi_1}\hat{\sigma}_{\Delta\Phi_2} \quad (16c)$$

with residual vector $\mathbf{v}_{P\Phi} = \left[v^1_{P\Phi} \quad v^2_{P\Phi} \quad \cdots \quad v^n_{P\Phi}\right]^{T}$ and STDs of $\hat{\sigma}_{\Delta\Phi_1}$ and $\hat{\sigma}_{\Delta\Phi_2}$ are calculated by (8).

Generation of the third frequency GPS signals

The DD P5 code observation is generated as,

$$\Delta P_5 = \Delta\rho + \Delta T + \frac{f_1^2}{f_5^2}\Delta I + \varepsilon_{\Delta P_5} \quad (17a)$$

where the true DD satellite-to-receiver range $\Delta\rho$ is computed with ephemeris and known precise receiver coordinates; ΔT and ΔI are calculated respectively by (4b) and (5b); DD code observation noise $\varepsilon_{\Delta P_5}$ consists of combined DD phase noises of $\varepsilon_{\Delta\Phi_1}$ and $\varepsilon_{\Delta\Phi_2}$ and randomly simulated noise ε_{SP},

$$\varepsilon_{\Delta P_5} = 4.32\varepsilon_{\Delta\Phi_2} - 5.32\varepsilon_{\Delta\Phi_1} + \varepsilon_{SP} \quad (17b)$$

where the combination coefficients of phase noises at L1 and L2 are calculated by $\frac{f_2^2\left(f_1^2 + f_5^2\right)}{f_5^2\left(f_1^2 - f_2^2\right)} \approx 4.32$ and $\frac{f_1^2\left(f_2^2 + f_5^2\right)}{f_5^2\left(f_1^2 - f_2^2\right)} \approx 5.32$ respectively; ε_{SP} is mainly used to compensate the noise at generated code measurements and normally distributed with mean zero and variance σ^2_{SP} is determined as,

$$\hat{\sigma}^2_{SP} = \sigma^2_{\Delta P_5} - 28.28\hat{\sigma}^2_{\Delta\Phi_1} - 18.64\hat{\sigma}^2_{\Delta\Phi_2} + 45.92\hat{\rho}_{\Phi_1,\Phi_2}\hat{\sigma}_{\Delta\Phi_1}\hat{\sigma}_{\Delta\Phi_2} \quad (17c)$$

where $\hat{\sigma}_{\Delta\Phi_1}$, $\hat{\sigma}_{\Delta\Phi_2}$ and $\hat{\rho}_{\Phi_1,\Phi_2}$ are computed by Eqs.(8) and (13) respectively; the DD L5 code STD ($\sigma_{\Delta P_5}$) can be determined in terms of the STDs of DD P1 and P2 previously as previously estimated by (16).

However, generating the DD L5 phase signals is much more complex. Firstly, the DD L5 signal, analogously with the generation of DD P5, is assumedly generated as follows,

$$\begin{aligned} \Delta\Phi_5 &= \Delta\rho + W - \lambda_5\Delta N_5 + \varepsilon_{\Delta\Phi_5} \\ W &= \Delta T - \frac{f_1^2}{f_5^2}\Delta I \end{aligned} \quad (18a)$$

where $\Delta\rho$, ΔT and ΔI are calculated in the same way as those in (17); W is referred to as "integrated delay" in this context for the convenience of following discussion. It is noticed that the sign of ionospheric delay at L5 is opposite to that at P5. The noise $\varepsilon_{\Delta\Phi_5}$ consists of combined phase noises at L1 and L2 and simulated random noise $\varepsilon_{S\Phi}$,

$$\varepsilon_{\Delta\Phi_5} = 0.226\varepsilon_{\Delta\Phi_1} - 1.226\varepsilon_{\Delta\Phi_2} + \varepsilon_{S\Phi} = \varepsilon_W + \varepsilon_{S\Phi} \quad (18b)$$

where the coefficients of $\varepsilon_{\Delta\Phi_1}$ and $\varepsilon_{\Delta\Phi_2}$ are calculated by $\frac{f_1^2\left(f_2^2 - f_5^2\right)}{f_5^2\left(f_1^2 - f_2^2\right)} \approx 0.226$ and $\frac{f_2^2\left(f_1^2 - f_5^2\right)}{f_5^2\left(f_1^2 - f_2^2\right)} \approx 1.226$ respectively. Therefore, the STD of the noise ε_W introduced by integrated delay at DD L5 is,

$$\sigma_W = \sqrt{0.05\sigma^2_{\Delta\Phi_1} + 1.5\sigma^2_{\Delta\Phi_2} - 0.55\rho_{\Delta\Phi_1,\Delta\Phi_2}\sigma_{\Delta\Phi_1}\sigma_{\Delta\Phi_2}} \quad (18c)$$

The relation of σ_W and cross correlation coefficients between L1 and L2 is presented in Fig.1 with assumption

of 1 cm STDs for both DD L1 and DD L2 measurements. As illustrated, the STD of the noise introduced by integrated delay at DD L5 is always larger than 1 cm for the cross correlation coefficient variation ranging from -1 to 1.

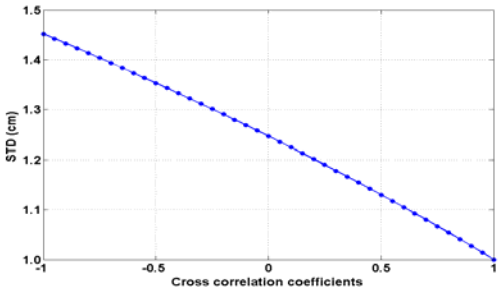

Fig.1. Relationship between the STD of error introduced at DD L5 and the cross correlation coefficients between L1 and L2 phases

In principle, it is desired to add random noise $\varepsilon_{S\Phi}$ to avoid correlation between the generated signal and original ones. Therefore the STD of noise at the generated DD L5 is calculated by,

$$\sigma^2_{\Delta\Phi_5} = \sigma^2_{S\Phi} + \sigma^2_W \qquad (18d)$$

where $\sigma_{S\Phi}$ is the STD of the added random noise $\varepsilon_{S\Phi}$. In fact, STDs of phase measurements at different frequencies are usually very close, but the STD of the noise ε_W introduced by integrated delay is larger than the STDs of DD L1 and L2 and it becomes much larger when the random noise $\varepsilon_{S\Phi}$ is added. Therefore the uncertainty of the integrated delay W must be reduced with filtering techniques such that its influence on DD L5 can be minimized. As a result, the DD L5 signal is practically generated as,

$$\Delta\Phi_5 = \Delta\rho + \tilde{W} - \lambda_5\Delta N_5 + \varepsilon_{\Delta\Phi_5} \qquad (19a)$$

where the filtered value $\tilde{W}$ is used instead of the calculated W, and the STD of $\tilde{W}$ can be considered as zero and thus $\sigma_{\Delta\Phi_5} = \sigma_{S\Phi}$. In this paper, the integrated delays W is fitted by a quadratic curve in a moving window over m epochs to minimize the random errors. The fitted values $\tilde{W}$ are used to generate DD L5 can be calculated by,

$$\tilde{\mathbf{W}} = \mathbf{A}\left(\mathbf{A}^T\mathbf{A}\right)^{-1}\mathbf{A}^T\mathbf{W} \qquad (19b)$$

where $\mathbf{A} = \begin{bmatrix} 1 & 1 & 1 \\ 1 & 2 & 2^2 \\ \vdots & & \\ 1 & m & m^2 \end{bmatrix}$, $\mathbf{W} = \begin{bmatrix} W_1 \\ W_2 \\ \vdots \\ W_m \end{bmatrix}$ and $\tilde{\mathbf{W}} = \begin{bmatrix} \tilde{W}_1 \\ \tilde{W}_2 \\ \vdots \\ \tilde{W}_m \end{bmatrix}$, and fitted residuals can be calculated by,

$$\mathbf{v} = \left(\mathbf{A}\left(\mathbf{A}^T\mathbf{A}\right)^{-1}\mathbf{A}^T - \mathbf{E}\right)\mathbf{W} \qquad (19c)$$

with **E** is m-by-m identity matrix. In this paper, the width of moving window is chosen to be 60 seconds, i.e., m=60 and the random noises are mostly removed such that we can ignore their influences. Thus, the STD of the added random noise $\varepsilon_{\Delta\Phi_5}$ can be directly and reliably determined by virtue of STDs of DD L1 and L2.

EXPERIMENT AND ANALYSIS

The dual-frequency GPS data were collected on Dec. 10th, 2006 from two CORS sites in Guangzhou of China where station spacing is approximately 51km and the station latitude is about 22°50′. These data sets were previously used by authors to assess the AR algorithm in severe ionosphere disturbance. 24 hours of data were collected with 1 second sampling rate and 15 degrees of mask angle. The L1, L2, C1 and P2 observations were available for the entire observation period. The programme is written in Matlab7.0 language to realize the semi-simulation method proposed in this paper.

The dual-frequency DD ambiguities are firstly fixed to their integer values by employing the wide-lane and ionosphere-free combinations with the precisely known reference station coordinates. The ionospheric delay and geometric error are then separated by (4b) and (5b) respectively and the result (DD ionospheric delay) is presented in Fig. 2. It is apparent that there is a significant ionospheric disturbance during the period from 4:00 to 9:00 in the GPS time, which corresponds to 12:00 to 17:00 in the local time. Apart from the disturbed region, the ionospheric delay series are smaller than 0.3m. Fig.3 shows a smaller segment of the DD L1 ionospheric delay result, GPS time 4:00 to 6:30, where the disturbance started. For both figures, each of the coloured lines represents result for different pair of GPS satellites available at that time.

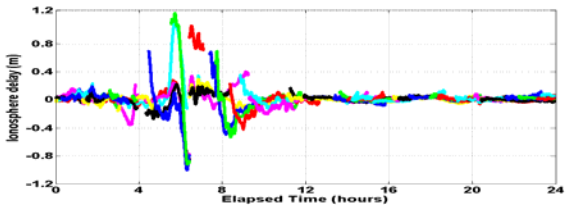

Fig.2. DD ionospheric delay series at L1

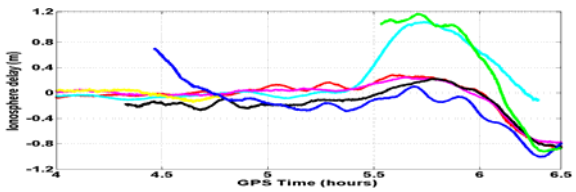

Fig.3. Variation of DD ionospheric delay for some pairs of DD satellites in the ionosphere disturbance period

A general tropospheric model is primarily applied to correct the original observation, and then the geometric error series calculated by (5b) are given in Fig. 4. The amplitude of the whole geometric error series is smaller than 5 cm except for some pairs of satellites with lower

elevation angles. It is observed that the geometric errors are seriously influenced by the variation of satellite elevation angles. For the given data set, the geometric error is smaller than 5 cm for all pairs of DD satellites with elevation angle higher than 15 degrees. Relationship of the geometric error variation and the elevation angle for one given pair of DD satellites (PRN 16 and PRN 31) is shown in Fig. 5. Obviously, the geometric error becomes larger with the decrease of elevation angle.

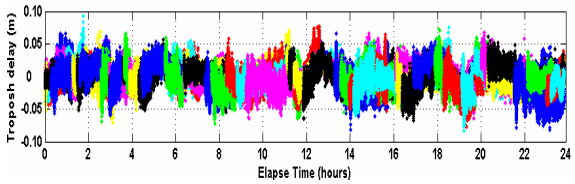

Fig.4. DD geometric error series

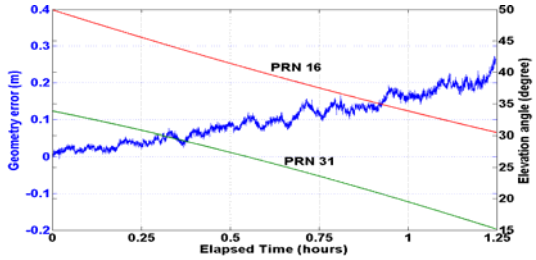

Fig.5. Relationship of geometric error and elevation angle

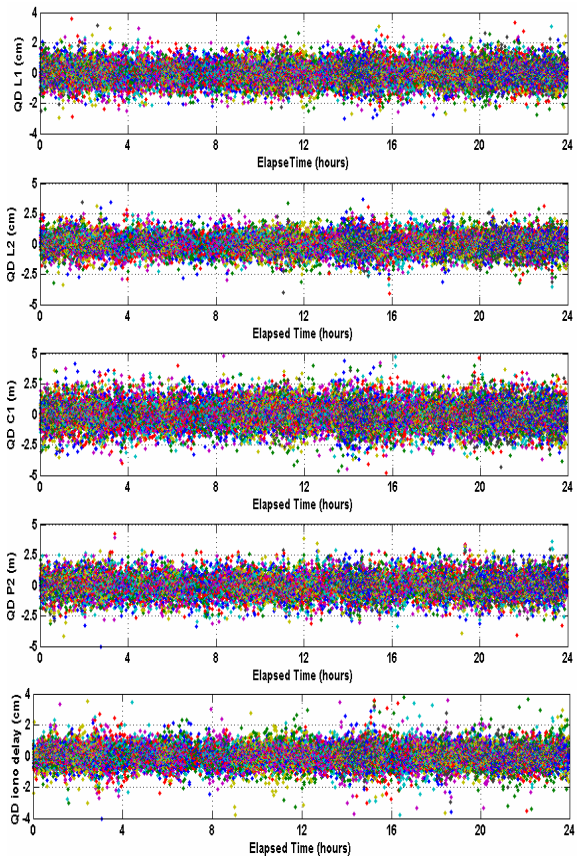

Fig.6. QD observation series respectively for L1, L2, C1, P2 and ionospheric delay

The QD series for L1, L2, C1, P2 and ionospheric delay are respectively presented in the Fig 6. It is obvious that all series are so random, which can also be verified by spectrum analysis proposed by Kim and Langley (2001). It is emphasized that the noises in QD series are enlarged by $\sqrt{6}$ times with respect to DD ones.

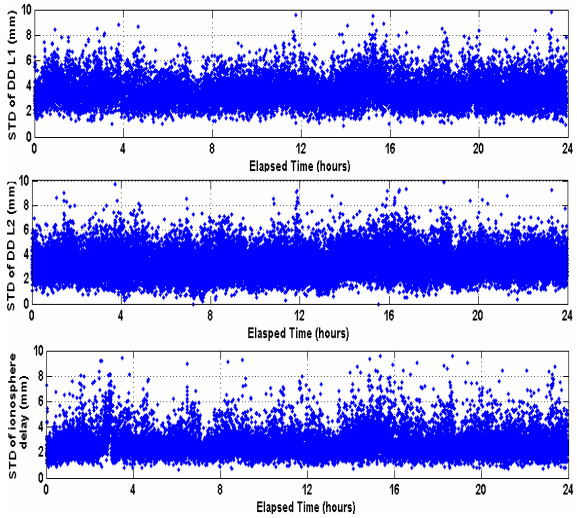

Fig.7. STD series of DD L1, DD L2 and DD ionospheric delay

Based on the QD observations, the STDs of DD L1, DD L2 and DD ionospheric delay are estimated according to the proposed procedure in Sect. 3 and the results are presented in Fig. 7. The STD series of DD C1 and DD P2 obtained from (16) are shown in Fig 8.

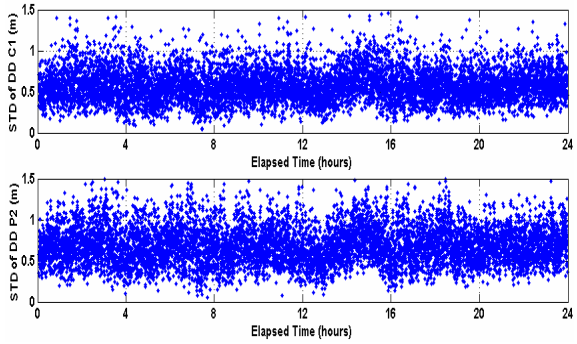

Fig.8. STD series of DD C1 and DD P2

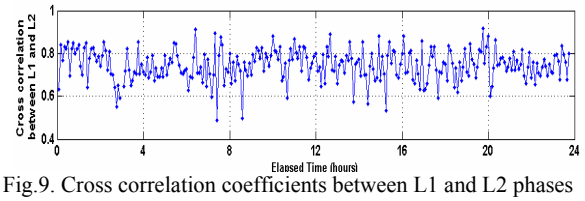

Fig.9. Cross correlation coefficients between L1 and L2 phases

In addition to the estimated STDs of DD phases and ionospheric delays, the cross correlation coefficients are estimated by (13) and averaged over every 5 minutes, illustrated in Fig. 9. It is seen that the cross correlation coefficients are obviously rather stable and the positive correlation with correlation coefficient of about 0.7 between L1 and L2 phases is really existent.

The variations of STDs of DD L1, DD L2 and DD ionospheric delay and the elevation angles for PRN 16 and PRN 31 satellites (the DD pair) are presented in Fig.10. It is evident that the STDs grow larger while the decrease of elevation angles. Therefore, the STDs of simulated noises at the generated signals should vary according to the elevation angles for different DD satellite pairs. However, the cross correlation coefficients for this DD satellite pair are relatively stable, as shown in Fig. 11, which reversely confirmed the existence of cross correlation.

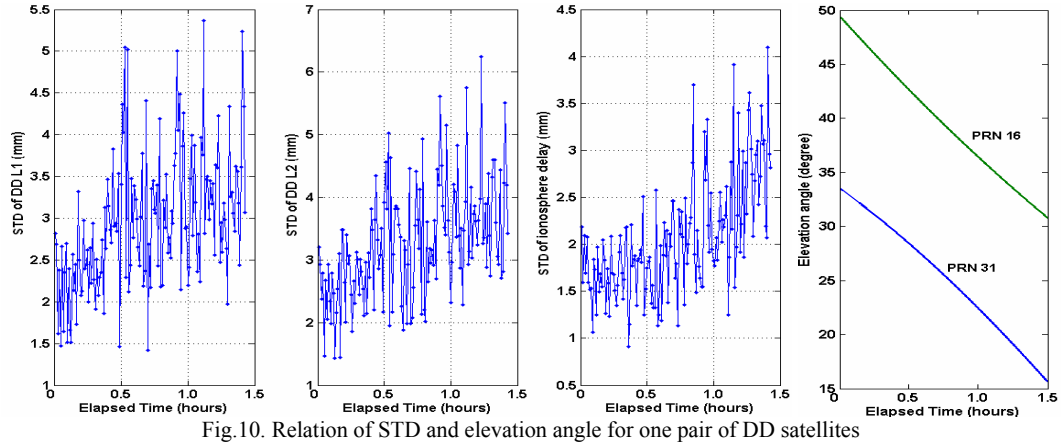

Fig.10. Relation of STD and elevation angle for one pair of DD satellites

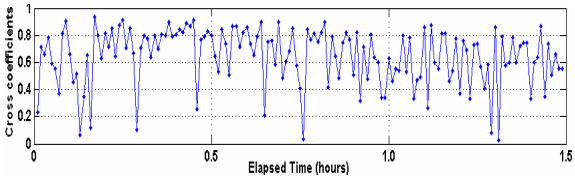

Fig.11. Cross correlation coefficients for one pair of DD satellites

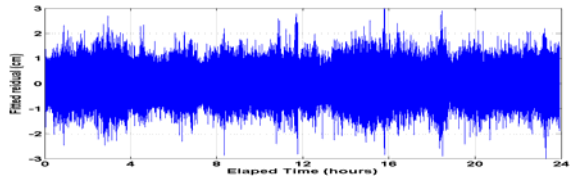

Fig.12. Fitted residuals of integrated delays

As mentioned above, the integrated delays, i.e. W in (18), are filtered by a quadratic curve fitting process to reduce the effects of phase random noises. The fitted residuals calculated by (19c) are shown in Fig.12. It illustrates that the magnitude of the residuals is very close with that of ε_W in (18c). This implies that the quadratic curve fitting is efficient for mitigating the effects of the random noises of integrated delays and thus reducing their uncertainties.

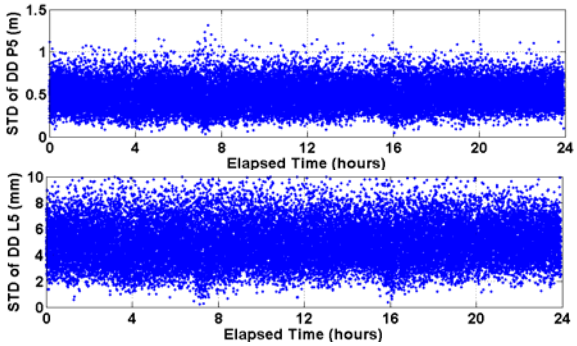

Fig.13. STD series of the generated DD P5 and L5

Based on the estimator series above, the uncertainties of code and phase at the third signals and the cross correlation, i.e., , $\sigma_{\Delta P_5}$, $\sigma_{\Delta\Phi_5}$ and $\rho_{\Delta\Phi_1,\Delta\Phi_2}$ are finally chosen to be 0.5 m, 5 mm and 0.7, respectively. As a result, σ_{SP} and $\sigma_{S\Phi}$ are reasonably determined. Finally, the new signals are generated according to the procedure proposed in this paper and their STDs are also assessed. The STDs of the generated DD P5 and DD L5 are illustrated in Fig. 13. As shown, the estimated STDs series are very close with the previously given values, which, in turn, proves the correctness of generated signals.

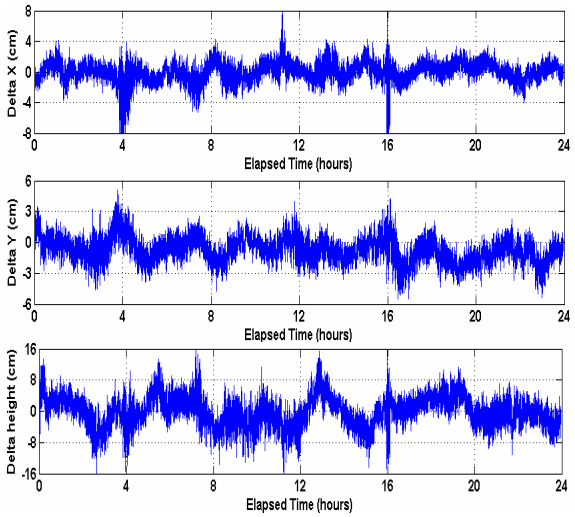

Fig.14. Positioning series based on ionosphere-free combinations of DD L1 and L5 phases

The positioning solutions are examined as well to further verify the correctness of the new generated signals. All positioning coordinates in WGS84 are transformed into horizontal and height components in the local coordinate

system and coordinate discrepancies are referred to the difference between estimated and precisely known coordinates. In order to exclude the influence of severe ionospheric delay, the ionosphere-free combined measurements between DD L5 and DD L1 are employed. As Fig. 14 shown, the horizontal coordinates are always smaller than 5 cm and the height components smaller than 10 cm, except some occasional disturbances. These results further validate the correctness of the generated DD phase signals.

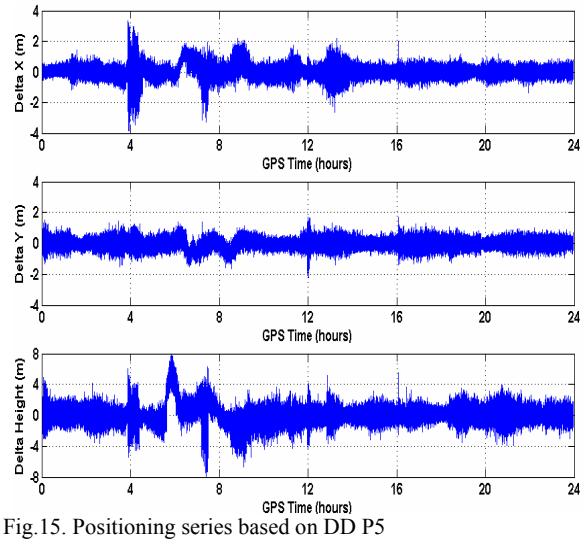

Fig.15. Positioning series based on DD P5

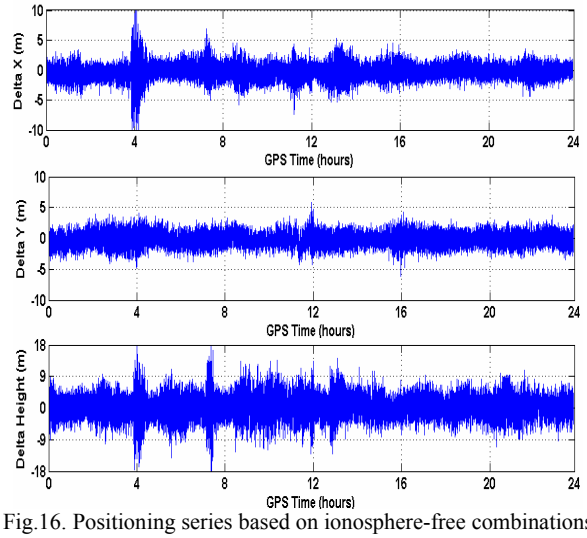

Fig.16. Positioning series based on ionosphere-free combinations of DD P5 and C1 codes

The positioning solutions from the generated DD P5 codes and their ionosphere-free combinations with DD C1 codes are also analysed. Fig. 15 shows the positioning results of sole DD P5 code and the height variation is shown to be seriously suffered from the ionospheric disturbance (see e.g. from 4:00 to 9:00 of GPS time in Fig. 15). The code based DD GPS positioning discrepancies using ionosphere-free combinations is presented in Fig.16. Comparing these two figures, the variation magnitude of positioning results based on the ionosphere-free combinations is enlarged despite the removal of ionosphere disturbances. This is caused by the fact that the code noises have been enlarged by about 3 times.

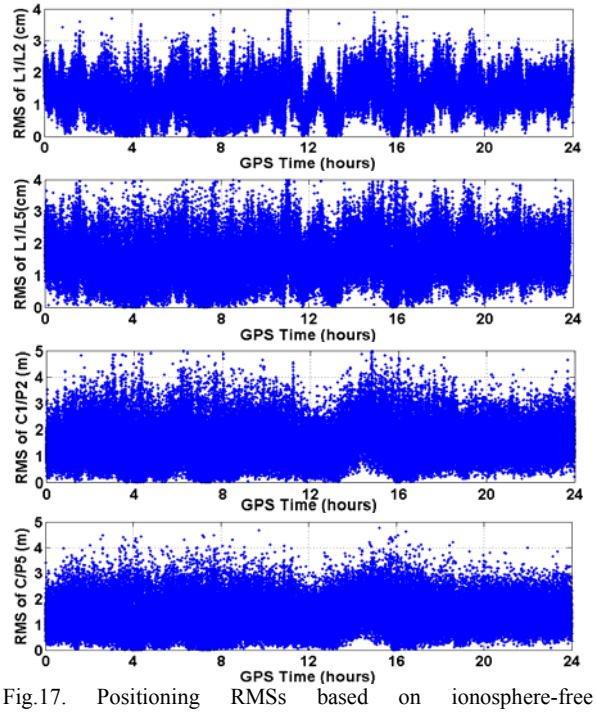

Fig.17. Positioning RMSs based on ionosphere-free combinations

In order to further verify the reliability of stochastic characteristics evaluation and the generated signals, the Root Mean Squares (RMS) of positioning are estimated based on ionosphere-free combinations of the DD L1 and L2 (L1/L2), DD L1 and L5 (L1/L5), DD C1 and P2 (C1/P2) and DD C1 and P5 (C1/P5). The results are illustrated in Fig. 17. As mentioned above, we have determined $\sigma_{\Delta\Phi_5}$, $\sigma_{\Delta P5}$ and $\rho_{\Delta\Phi_1,\Delta\Phi_2}$ to be 5mm, 0.5m and 0.7, and $\sigma_{\Delta\Phi_1} = \sigma_{\Delta\Phi_2} \approx 5\text{mm}$, $\sigma_{\Delta C1} = \sigma_{\Delta P2} \approx 0.5\text{m}$ for signal generation. In principle, the theoretical RMS of L1/L2 is determined by,

$$\sigma_{L1/L2} = \frac{\sqrt{f_1^4\sigma_{\Delta\Phi_1}^2 + f_2^4\sigma_{\Delta\Phi_2}^2 - 2\rho_{\Delta\Phi_1,\Delta\Phi_2}\sigma_{\Delta\Phi_1}\sigma_{\Delta\Phi_2}}}{f_1^2 - f_2^2} \approx 9\text{mm} \quad (20)$$

Similarly, $\sigma_{L1/L5}$, $\sigma_{C1/P2}$ and $\sigma_{C1/P5}$ can be theoretically determined to be 1.3cm, 1.49m and 1.3m, respectively. According to the results in Fig.17, the mean RMSs can be calculated to be 1.3cm, 1.5cm, 1.55m and 1.37m for L1/L2, L1/L5, C1/P2 and C1/P5 respectively. Comparing the calculated RMSs with the theoretical values, results are very similar with calculated RMSs and have slightly higher value. This may be caused by the residual geometric errors in ionosphere-free combinations.

We now can use the "real" triple frequency data to test TCAR algorithms, which also reversely validate the generated data. Three additional 24-h GPS data sets sampling at 1 second were collected from the US CORS

(http://www.ngs.noaa.gov/CORS) on the 1st of Feb., 2008. For each baseline, the third phase and code signals were firstly generated using the proposed procedure. The overall AR success rate, which is defined as the ratio of the total number of epochs with all correct ambiguity fix to the total number of epochs, is computed. We test the geometry-based TCAR models proposed by Feng (2008), which chooses some ionosphere-reduced virtual signals and models for AR. As given in Table 1, three baselines are of length approximately 15km, 53km and 78km respectively. The first column gives the modelling schemes, where $\Delta P_{(0,1,1)}$-$\Delta\Phi_{(0,1,-1)}$ and $\Delta P_{(1,1,0)}$-$\Delta\Phi_{(1,-1,0)}$ represent the geometry-free process and all of the rest represent the combined signals used together in geometry-based AR mode; ΔP_{IF} represents the ionosphere-free combination of DD P1 and P2 and $\Delta P_{(1,1,0)}$ is the narrow-lane combination of the DD P1 and P2. One can be referred to Feng (2008) for detailed characteristics of these virtual signals. The table clearly confirms the best AR performance of the two EWL signals $\Delta\Phi_{(0,1,-1)}$ and $\Delta\Phi_{(1,-6,5)}$ with respect to other options in the same category. For the NL AR, the lower AR success rate for the 78km baseline may be mainly caused by the effect of systematic tropospheric errors, which is around 0.5 cycles.

Table 1. Success rate of TCAR

Combined observation	Success rate of AR (%)		
	15km	53km	78km
$\Delta P_{(0,1,1)}$-$\Delta\Phi_{(0,1,-1)}$	100	100	100
$\Delta P_{(1,1,0)}$-$\Delta\Phi_{(1,-1,0)}$	84.09	91.21	93.05
$\Delta\Phi_{(1,-6,5)}$, $\Delta P_{(1,1,0)}$	100	100	100
$\Delta\Phi_{(1,-5,4)}$, $\Delta P_{(1,1,0)}$	100	99.96	100
$\Delta\Phi_{(1,-4,3)}$, $\Delta P_{(1,1,0)}$	99.77	99.65	100
$\Delta\Phi_{(1,-3,2)}$, $\Delta P_{(1,1,0)}$	99.04	98.77	99.95
$\Delta\Phi_{(1,-6,5)}$, ΔP_{IF}	90.08	94.82	99.07
$\Delta\Phi_{(4,0,-3)}$,$\Delta\Phi_{(1,0,-1)}$	99.23	88.48	34.88
$\Delta\Phi_{(4,-3,0)}$,$\Delta\Phi_{(1,-1,0)}$	99.67	89.84	34.68
$\Delta\Phi_{(4,-1,-2)}$,$\Delta\Phi_{(1,0,-1)}$	99.39	88.38	32.84

CONCLUDING REMARKS

This paper has developed a new approach, semi-simulation method, for generating the third frequency DD measurements using the real GPS dual-frequency data, consisting of three steps. Firstly, the dual-frequency GPS data are processed on a baseline basis by means of the network-based RTK concept and the effects of ionospheric delays and geometric errors are separated. Secondly, a multiple difference based method is applied to assess the uncertainties of code and phase observations as well as the cross correlation between L1 and L2 phases, which contribute to the simulation of the random noise at the generated signals. In the third step, the third frequency DD P5 is generated according to the proposed procedure based on the separated errors and their corresponding STDs obtained from the real dual-frequency GPS measurements. However, as the DD L5 phase generation is much complex than that of the DD P5, the estimated ionospheric delays and geometric errors have to go through a filtering process or quadratic curve fitting in a moving window to reduce the effects of random noises. Otherwise, the uncertainties of the generated DD L5 signals will be much larger than the real scenarios.

A dual-frequency GPS data set with severe ionospheric disturbance is firstly processed to show the whole proposed procedure. The positioning results have shown consistency between the generated signals and the real world dual-frequency scenarios. Three additional dual-frequency GPS data sets have also been examined and the generated signals have been used to evaluate the geometry-based TCAR success rate performance. Testing results have demonstrated consistency with the theoretical. On all account, the proposed approach is rather convenient and efficient for generation of new DD signals based on the existing dual-frequency GPS signals, benefiting GNSS research and development for future generation GNSS technology and applications.

ACKNOWLEDGEMENTS

This work is partially supported by Cooperative Research Centre for Spatial Information (CRCSI) project 1.4 for regional GNSS positioning awarded to Higgins and Feng from 2007 to 2010, and partially supported by the National Science Foundation of China (Grant No.: 40674003). The author would also like to thank A/Prof. Yanming Feng from Queensland University of Technology, Australia, for his generous support, thoughtful comments. The author is grateful to Prof. Yunzhong Shen from Tongji University, China for his advice and support. Last but not least, Dr. Charles Wang is appreciated for polishing manuscript.

REFERENCES

Cao W., O'Keefe K., Elizabeth Cannon M. (2007) Partial ambiguity fixing within multiple frequencies and systems, In: Proceedings of ION GNSS 20th International Technical Meeting of the Satellite Division, 25-28, Sept., Fort Worth, TX, pp: 668-678

Chen W., Hu C., Chen Y., Ding X., Kwok S. (2001) Rapid static and kinematic positioning with Hong Kong GPS active network, In: Proceedings of ION GPS 2001, 11-14 Sept., Salt Lake City, UT, pp:346-352

Feng Y., Rizos C. (2005) Three carrier approaches for future global, regional and local GNSS positioning services: concepts and performance Perspectives, In: Proceedings of ION GNSS 2005, 13-16 Sept., Long Beach, CA, pp: 2277-2787

Feng Y. (2008) GNSS three carrier ambiguity resolution using ionosphere-reduced virtual signals, J Geod, DOI 10.1007/s00190-008-0209-x

Forssell B., Martin-Neira M., Harris R. (1997) Carrier phase ambiguity resolution in GNSS-2, In: Proceedings of ION GPS-97, 16-19 Sept., Kansas City, pp: 1727-1736,

Frei E., Beulter G. (1990) Rapid static positioning based on the fast ambiguity resolution approach 'FARA': theory and first results, Manuscr Geod, 15:326–356

Hatch R. (1990) Instantaneous ambiguity resolution, Proceedings of KIS'90, 10-13 Sept., Banff, Canada, pp: 299-308

Hatch R., Jung J., Enge P., Pervan B. (2000) Civilian GPS: the benefits if three frequencies, GPS Solut, 3(4):1-9

Hu G., Khoo H., Goh P., Law C. (2003) Development and assessment of GPS virtual reference stations for RTK positioning. J Geod, 77:292-302

Ji S., Chen W., Zhao C., Ding X., Chen Y. (2007) Single epoch ambiguity resolution for Galileo with the CAR and LAMBDA methods, GPS Solut, 11:259-268

Kim D., Langley R. (2001) Estimation of Stochastic Model for Long-Baseline Kinematic GPS Applications, In: Proceedings of ION National Technical Meeting, 22-24 Jan., Long Beach, CA, USA, pp: 586-595

Kim D., Langley R. (2007) Long-range single-baseline RTK for complementing network-based RTK, In: Proceedings of ION GNSS 20th International Technical Meeting of the Satellite Division, 25-28, Sept., Fort Worth, TX, pp: 639-650

Li B., Shen Y. (2008) Optimal combination of Galileo inter-frequencies, In: Xu P., Liu J., Sermanis A. eds. International Association of Geodesy Symposia: VI Hotine-Marussi Symposium on Theoretical and Computational Geodesy, 29 May-2 Jun., 2006, Wuhan, China. Springer Berlin Heidelberg, (132):195-199

Li B., Shen Y., Xu P. (2008) Assessment of the stochastic model for GPS measurement with different types of receivers, Chinese Science Bulletin (in press)

Park C., Kim I., Lee J.G., Jee G.I. (1996) Efficient ambiguity resolution using constraint equation, In: Proceedings of IEEE PLANS, Position Location and Navigation Symposium, pp: 277-284

Schaffrin B., Grafarend E. (1986) Generating classes of equivalent linear models by nuisance parameter elimination, applications to GPS observations, Maunscr Geod, 11:262-271

Shen Y., Li B. (2007) Regularized solution to fast GPS ambiguity resolution, J. Surv. Eng., 133(4): 168-172

Shen Y., Xu G. (2008) Simplified equivalent representation of differenced GPS observation equations, GPS Solut, 12 (2): 99-108

Teunissen P. (1994) A new method for fast carrier phase ambiguity estimation, IEEE PLANS'94, Las Vegas,11-15 April, pp: 562-573

Teunissen P., Joosten P., Tiberius C. (2002) A comparison of TCAR, CIR and LAMBDA GNSS ambiguity resolution, In: Proceedings of ION GPS, 24-27 Sept. Portland, Oregon, pp: 2799-2808

Vollath U., Birnbach S., Landau H. (1998) Analysis of three carrier ambiguity resolution(TCAR) technique for precise relative positioning in GNSS-2, In: Proceedings of ION GPS98, 15-18 Sept., pp: 417-426.

Wener W., Winkel J. (2003) TCAR and MCAR options with Galileo and GPS, In: Proceedings of ION GPS/GNSS 2003, 9-11 Sept., Portland, OR, USA, pp: 790-800

Xu P. (2006) Voronoi cells, probabilistic bounds, and hypothesis testing in mixed integer linear models, IEEE Transactions on Information Theory, 52 (7):3122-3138

Zhang J., Lachapelle G. (2001) Precise estimation of residual tropospheric delays using a regional GPS network for real-time kinematic applications, J Geod, 75: 255-266